The Journal of Engine Research

Journal Homepage: www.engineresearch.ir

# Evaluating the coupled thermo-mechanical stresses for an aluminum alloy piston used in a gasoline engine XU7

H. Golbakhshi[1*], M. Namjoo[2], M. Dowlati[3], F. Khoshnam[4]

[1,2,3,4] *University of Jiroft , Jiroft, Iran*
*Corresponding Author , golbakhshi@ujiroft.ac.ir*

**ARTICLE INFO**

*Article history:*
Received: 26 October 2015
Accepted: 1 March 2015

*Keywords:*
Piston
Finite Element Method
Thermo-mechanical analysis
Ceramic Coating
Stress distribution

**ABSTRACT**

In the modern engines with higher compression ratios, severe pressures and non-uniform heating up is occurred for the engine parts. The piston as the most critical part among all automotive components has been the subject of numerous studies on calculation of temperature distribution, but thermal stress analyses are limited. In this study, the piston of gasoline engine XU7 which is widespread in Iran transport section is considered for thermo-mechanical investigation. A 3D linear static stress analysis is constructed in COSMOS Works to determine the stress distribution during the combustion stroke. The maximum normal stress takes place at the middle surface of the piston crown. The von Mises stress is found to be critical on upper parts of the pin-hole area. Effect of ceramic coating layer on stress distributions are evaluated and compared with results obtained for a traditional uncoated piston. According to the results, the maximum stress can be readily controlled by increasing the thickness of ceramic layer.

## 1) Introduction

The engine piston as the movable wall of the combustion chamber is affect by high pressure and temperature resulted from explosion of air-fuel mixture which may reach about 180-200 bar for diesel engines and less than 70 bar for gasoline engines [1]. It is noted that the components subjected to high temperatures lose their stiffness and strength due to decrease in amount of Young modulus and yield point [2]. Temperature distribution also leads to further thermal deformations and thermal stresses and has a crucial role in amount of generated frictional effects on the piston skirt region [3]. So, the piston should be well designed to withstand the thermal and mechanical stress resulted from extreme heat and pressure of the combustion chamber.

In modern engines, the desire to increase thermal efficiency makes it tempting to adopt higher compression ratios [4]. It seems an appropriate strategy for promoting the older engines like XU7 with widespread use in Iran. However, severe resulted heat and pressure in the combustion chamber should be considered so that the hardness and strength of the parts would not be destructively affected [5].

Computer simulations of the piston are very useful and economically viable for reducing the time and cost at design stage of the engine before the first prototype is constructed. There are many research papers on the calculation of temperature distribution. Cerit and Soyhan showed that the maximum temperature on the top surface of aluminum and steel coated with ceramic layer may diminish and, compared to the clean piston [6]. Using a three dimensional finite element model, Li [7] proved that the operating temperatures on skirt region play an important part in reduction of scuffing and friction. Tahar Abbes et al. [8] presented the thermo-mechanical behavior of a direct-injection diesel engine piston subjected to the combined thermal and mechanical loads. Bohac et al. [9] used a resistance-capacitance model for steady state and transient heat transfer of gasoline engines. Using Matlab software, Ghasemian and Jazayeri evaluated the effect of cooling system performance on temperature distribution of a specified gasoline engine [10]. Gharloghy and Kakaee successfully investigated the effect of boundary conditions and rings on temperature distribution of an EF7TC engine [11]. Pourhamid et al. showed that the pistons and cylinders made of combination ceramics and metals, known as functionally graded materials, have better wear properties and thermal insulations [12].

Thermal ceramic coatings are commonly applied to insulate the substance surfaces to allow for higher operating temperatures and protecting the metallic surfaces from thermal stresses during the power and exhaust strokes of both diesel and gasoline engine cycles [13, 14]. However, one of the main characteristics of the ceramics is brittleness and residual thermal stress leads to spallation of coatings [15].Therefore, it is very important to determine the thermal and mechanical stresses occurred in the piston for instantaneous heating and cooling the piston. However, thermo-mechanical stress analyses for the engine pistons are limited [1].

In this paper, a thermo- mechanical investigation is presented for evaluating the stress distribution of an aluminum piston assembled in XU7 gasoline engine. Several thicknesses of ceramic layers are studied to achieve the optimum engine performance. The results are then compared with the results of the uncoated piston to evaluate the contribution of coating layer to better engine performance. The effect of thermal condition of lubricating oil on stress and deformation fields of the engine piston is also investigated in this work.

## 2) Material and method

The object of the study is taken from the piston of gasoline engine XU7. This engine is assembled in car Peugeot 405 as a widespread car in Iran transport section. The characteristics of the engine under study are summarized in Table 2. The rings placed in piston grooves aid in sealing the cylinder to prevent the escape of exploded gases. Piston and rings are made of AlSi alloy and cast iron, respectively. The materials used in the analysis are assumed to be linear elastic and isotropic and their mechanical properties are given in Table 1.

In order to calculate the thermal stress distribution in the piston as a complex shaped thick-walled cylinder and variable thickness, the equilibrium equation in polar coordinate is consider [16]:

$$\frac{1}{r}\frac{\partial}{\partial r}\left(r\sigma_r\right)+\frac{1}{r}\frac{\partial\tau_{r\theta}}{\partial\theta}+\frac{\partial\tau_{rz}}{\partial z}-\frac{\sigma_\theta}{r}=0 \quad (1)$$

$$\frac{1}{r}\frac{\partial}{\partial r}\left(r\tau_{r\theta}\right)+\frac{1}{r}\frac{\partial\sigma_\theta}{\partial\theta}+\frac{\partial\tau_{\theta z}}{\partial z}=0 \quad (2)$$

$$\frac{1}{r}\frac{\partial}{\partial r}\left(r\tau_{rz}\right)+\frac{1}{r}\frac{\partial\tau_{\theta z}}{\partial\theta}+\frac{\partial\sigma_z}{\partial z}=0 \quad (3)$$

Which the stresses are determined as follows:

$$\sigma_r=\frac{2G}{1-2\nu}\left[\left(1-\nu\right)\varepsilon_r+\nu\left(\varepsilon_\theta+\varepsilon_z\right)\right] \quad (4)$$

$$\sigma_\theta=\frac{2G}{1-2\nu}\left[\left(1-\nu\right)\varepsilon_\theta+\nu\left(\varepsilon_r+\varepsilon_z\right)\right] \quad (5)$$

$$\sigma_z=\frac{2G}{1-2\nu}\left[\left(1-\nu\right)\varepsilon_z+\nu\left(\varepsilon_r+\varepsilon_\theta\right)\right] \quad (6)$$

$$\tau_{r\theta}=G\gamma_{r\theta} \quad (7)$$

$$\tau_{rz}=G\gamma_{rz} \quad (8)$$

$$\tau_{z\theta}=G\gamma_{z\theta} \quad (9)$$

However, it is noted that the total strain are made of two strains, the first one is dependent on the induced stresses and other one is due to free thermal expansion. Thus, evaluating the temperature distribution is a key factor in thermo-elastic analysis of engine piston. The differential equation of time dependent heat flow is given in polar coordinate by:

$$\frac{1}{r}\frac{\partial}{\partial r}\left(kr\frac{\partial T}{\partial r}\right)+\frac{1}{r}\frac{\partial}{\partial \theta}\left(kr\frac{\partial T}{\partial \theta}\right) +\frac{\partial}{\partial z}\left(k\frac{\partial T}{\partial z}\right)=\frac{1}{\alpha^{*}}\frac{\partial T}{\partial t} \quad (10)$$

where $\alpha^{*}$ is the thermal diffusivity, $r$ is the radial distance and $T$ is the temperature as a function of $r$ and $t$.

A closed form solution of the coupled set of differential equations is commonly difficult to obtain. So, the analysis should be performed by numerical approaches like the finite element method.

For the steady state thermal analysis of the piston, the major mechanism for heat transfer is convection. In this paper, the fluid temperature $T_f$ and the convection coefficient $h$ are considered as the boundary conditions of the problem. These conditions can be mathematically expressed as follows:

$$-k\frac{\partial T}{\partial n}=h\left(T-T_f\right) \quad (11)$$

where $n$ is the exterior normal vector for the boundaries.

Table 1: Material properties of piston, ring and ceramic [1].

| | AlSi | Steel | NiCrAl | $MgZrO_3$ | Oil ring | Compression ring |
|---|---|---|---|---|---|---|
| Thermal conductivity, [W/m °C] | 155 | 79 | 16.1 | 0.8 | 33 | 52 |
| Thermal expansion, $10^{-6}$ [1/°C] | 21 | 12.2 | 12 | 8 | 12 | 10 |
| Density, [kg/m$^3$] | 2700 | 7870 | 7870 | 5600 | 7200 | 7300 |
| Specific heat, [J/kg°C] | 960 | 500 | 764 | 650 | | |
| Poisson's ratio | 0.3 | 0.3 | 0.27 | 0.2 | 0.29 | 0.3 |
| Young's Modulus , [GPa] | 90 | 200 | 90 | 46 | 142 | 125 |

According to the empirical investigations [17-19], the heat transfer coefficients are greatly dependent on properties of coolant, the speed of engine and thermodynamic conditions of combustion gases. On 5000 rpm, maximum power condition and partially dry lubrication is provided for the engine. So, this speed is considered for the analysis. Based on the published literatures [20-23], it is reasonable to estimate the inside ambient temperature as the average temperature values during an engine cycle [20].

Table 2: Specification of the engine under study

| | |
|---|---|
| Bore | 9.2 cm |
| Stroke | 8.9 cm |
| Compression ratio | 8.7 |
| Connecting rod | 13.61 cm |
| IVO | 34° bTDC |
| IVC | 74° aBDC |
| EVO | 36° bBDC |
| IP | 0.83 bar |
| IT | 297 K |
| $\lambda$ | 1.1 |
| RPM | 3000 |
| Ignition time | 55 bTDC |

For the considered case study, the average temperature and convection coefficients on each position of the piston are given in table 3. In this study the rings are considered to be in contact with both surfaces of ring gaps. When the clearance between piston and cylinder are high, formation of cavitation in lubricating oil film is inevitable. As result, the heat transfer conditions in this region are badly affected. Neglecting the effect of piston motion in the oil film thickness, it is assumed that the rings and skirt are fully engulfed in oil and there is no cavitation.

Table 3: Heat transfer coefficients and average temperature on each position of the piston [20-23].

| Region | Heat transfer coefficient ($\frac{w}{m^2K}$) | Average temperature of medium (℃) |
|---|---|---|
| The top of piston crown | 800 | 650 |
| The lateral surfaces of ring grooves | 280 | 300 |
| The regions between ring grooves | 200 | 160 |
| The piston skirt and pin-hole region | 400 | 120 |
| Internal oil-cooled regions of the piston | 1500 | 95 |

As previously mentioned, by improving the temperature distribution, the generated stresses can be effectively controlled. Developing high strength, heat resistance compounds of sprayed powders with the parent metals is a very important method to solve the problem of repair, reconditioning and increasing the service life of the engines [24]. The ceramic coating layers are commonly applied to the top of piston substrate metallic surfaces to insulate them thermally so as to allow for higher operating temperatures. To keep the combustion chamber volume constant, a layer having a certain thickness should be removed from the top surface of standard piston. The zirconia-based ceramic coating MgZrO3 is used as thermal barrier layer for piston coating. The low conductivity and relatively high coefficients of thermal expansion, greatly reduce the detrimental interfacial stresses. The bond coat layer, as an inter-metallic alloy, is first placed between the ceramic layer and the metal substrate for providing the adhesion of the coating layer to the substrate and reducing the internal stresses arisen from thermal shock. It is noted that the coefficient of thermal expansion of the bond coat should be between that of the ceramic layer and the metal substrate [25]. Then zirconia-based ceramic coating $MgZrO_3$ ranging in a thickness from 0.2 to 0.8 mm, are used as thermal barrier coatings owing to their low conductivity and their relatively high coefficients of thermal expansion, which reduced the detrimental interfacial stresses. The coating is also composed of a 0.1 mm NiCrAl as bond layer, which is deposited onto the piston crown by air plasma spraying technique [14]. Material properties of the $MgZrO_3$, NiCrAl and piston material made of AlSi alloy are listed in Table 1.

Thermal and stress analyses have been carried out by means of finite element method which is a powerful numerical method. Figure 1 show the solid model of the piston and cylinder under study which are generated by SolidWorks. As can be seen, great attention was paid for modelling the details of the parts. A commercial finite element package COSMOS, which has the capability of 3D heat transfer and stress analyses, is used for the current study. Uniform shapes and forms of elements play an important role to obtain precise results. Therefore, meshing of the piston is built with second order solid elements having 20 nodes for both thermal and structural fields. These elements can tolerate irregular shapes of the piston model. However, for the coating layers as narrow domains, the conventional automatic meshing with uniform distributed nodes usually yields ill-shaped elements in the bowl rim where the curvature of domain boundary is high. In order to avoid these ill-shaped elements, the boundary nodes distributed over the coating layers are manually adjusted. Resultantly, the finite element mesh of the piston shown in Fig. 1e, contains 176702 nodes and 860841 elements for improving the accuracy and acceptability of the obtained results.

The selection of the displacement boundary condition is very important to the finite element analysis. If the selection is not correct, it will seriously affect the calculation precision. On the moment of the maximum gas pressure, the pin contacted mainly to the upper surface of the pin hole, but the support reaction of the pin hole didn't act on the whole upper surface. In the cylindrical coordinate system, the displacements of X, Y directions of all nodes in the contact region were restricted. Moreover, by including the of cylinder model in the analysis, the displacements of Z direction on lateral side of piston pin boss were also restricted.

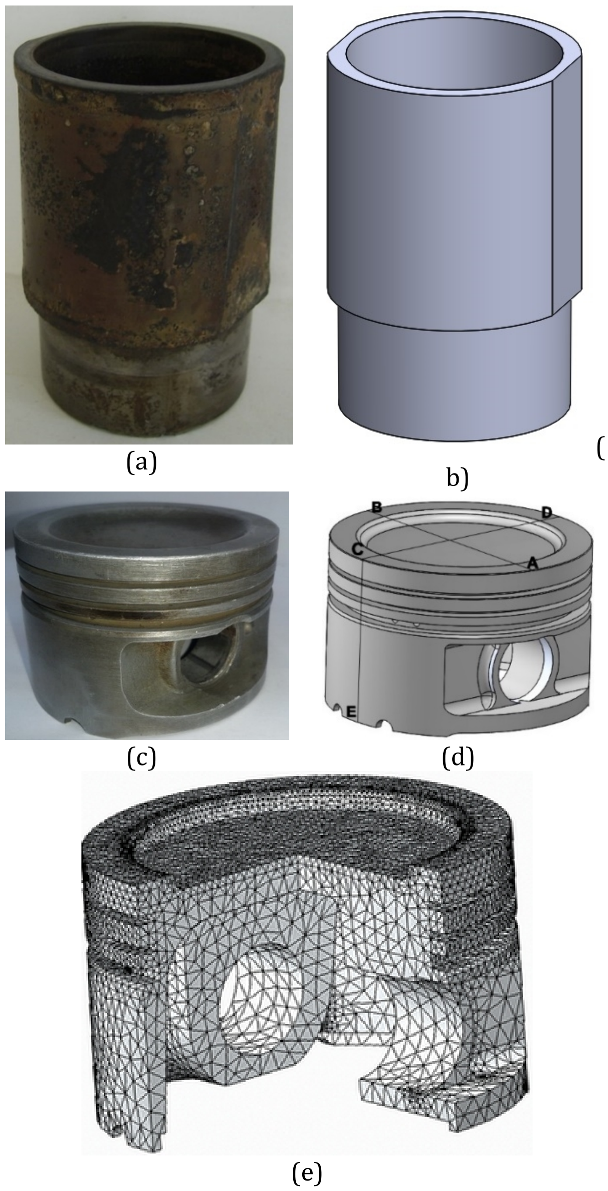


Figure 1: The models used in FE analysis: a and c) Images of the traditional piston and cylinder, b and d) Piston and cylinder solid models generated by SolidWorks and e) Finite element model of the piston

## 3) Result and discussion

The mechanical loads on the piston include gas pressure, reciprocating inertial force, side pressure, thermal load and support reaction on the inner surface of the pin hole In order to avoid neglecting any combination of forces that may be critical, the times at which individual components of the mechanical load reach a maximum are analyzed. In the current study, the maximum of cylinder pressure is at upper dead center at explosion stroke is considered for investigation [26]. The explosive pressure of fuel gas is the main factor to cause the stress concentration and the deformations are most serious at this moment. In addition, the side pressure on the skirt was zero at this moment. The values of gas pressures which are loaded on the piston top surfaces and ring grooves are listed in Table 4 [27]:

Table 4. Gas pressure of fire on the each position of the piston (MPa)

| | |
|---|---|
| Piston top, field of fire, upper and under surface of the first ring groove | 7.5 |
| Bottom Surface of the First Ring Groove | 5.7 |
| First piston land, upper and under surface of the second ring groove | 1.875 |
| Bottom Surface of the Second Ring Groove | 1.5 |
| Second piston land, upper and under surface of the third ring groove | 0.75 |
| Bottom Surface of the Third Ring Groove | 0.57 |
| Third piston land, upper and under surface of the fourth ring groove | 0.375 |
| Bottom surface of the fourth ring groove | 0.285 |

It is noted that the thermal conditions on different parts of the piston are significantly different. So, the temperature gradient would be unavoidable which may have affects the stress field. Ceramic coatings on the piston crown surface improves the temperature distribution and resultantly controls the thermal stresses and deformations within acceptable level [14]. However, ceramic layers may have limited life at any point where maximum thermal stress occurs [15]. In this study, the thermal stress distribution of engine piston is analyzed for evaluating the effect of ceramic layer thickness on amount of generated thermal stresses.

Distribution of normal stress, which may cause surface cracks in the coating, for various thicknesses are plotted in Figure 2.

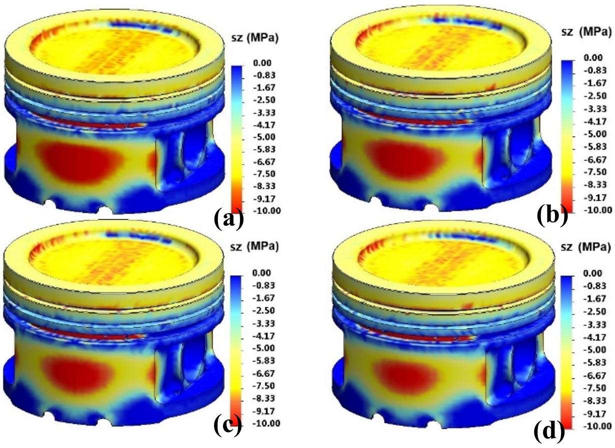


Figure 2: Normal stress distribution for four different coating thicknesses: a) 0.2, b) 0.4, c) 0.6 and d) 0.8 mm respectively

The maximum normal stresses occur at the top of piston crown surface and skirt region. It is obvious that the maximum stress over the ceramic top surface, which causes surface cracks, has a slight increase with increasing coating thickness. However, the magnitude of normal stresses on the skirt, reduce for thicker coating layers. The results of Zhao [28] proves the fact that the thermal stress under the ring groove of the ceramic coated piston is obviously less than that of the conventional piston. So, without any dangerous effect on ceramic layer, the normal stress distribution can be conveniently improved.

Distribution of shear stress on the crown and skirt regions of the piston, are shown in Figure 3.

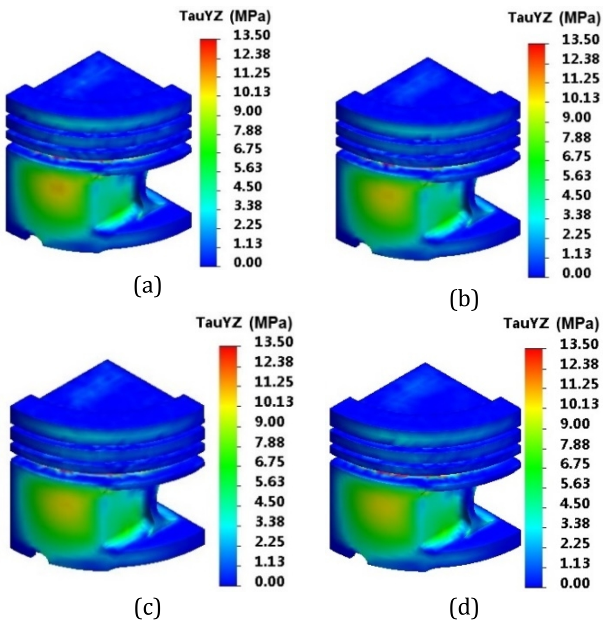


Figure 3: Distribution of shear stress for four different coating thicknesses: a) 0.2, b) 0.4, c) 0.6 and d) 0.8 mm respectively

The shear stress on the skirt can be interpreted as resisting effect against piston reciprocal motion. It is noted from the figures that a negligible increase in the shear stress is occurred for thicker ceramic layers. Meanwhile, amount of stresses on the skirt undergo a very slight reduction due to the contributing effect of ceramic layer on thermal strains of piston lower parts. According to obtained results for gradient of stress distributions over the surface ceramic layer, the most critical stresses are found along two perpendicular axes, one of them crossing the pin holes. For more quantitative investigations, several test points are chosen along the two axes shown in Figure 1d. For two testing paths AB and CD, the changing curves of normal stress for the conventional uncoated and ceramic coating piston are presented in Figures 4a and 4b. Similar results are obtained by Cerit, and Coban [13] for a diesel engine. Their results show that the maximum normal stress which occurs at the edges of piston crown is decreased by 19.6% for the thickness of 0.4 mm; while 15.8% decrease is found the current study for the same thickness.

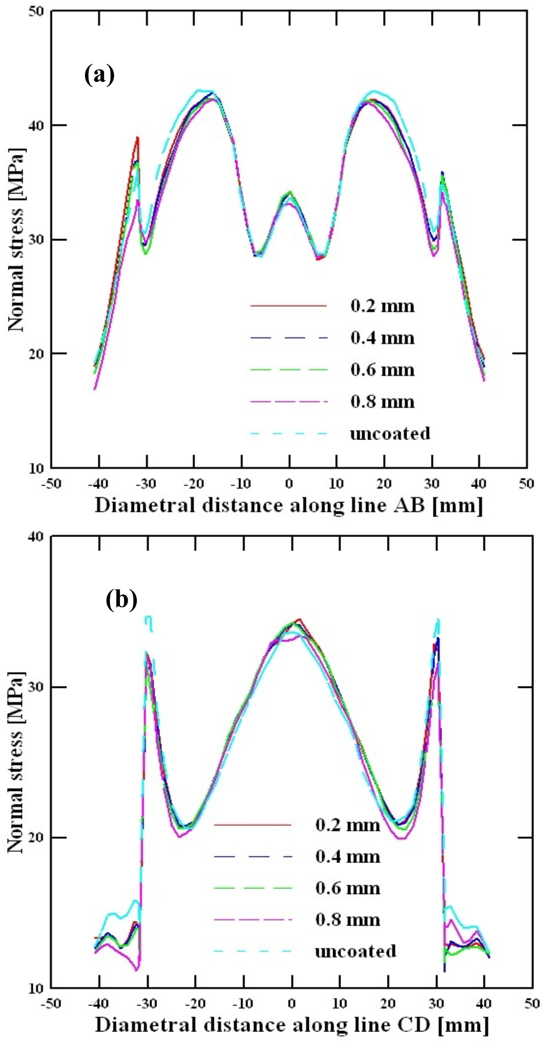


Figure 4: Variation of normal stresses along axes AB and CD over the piston crown surface

It can be concluded through analysis that the normal stress along the pin-holes axis, are much greater than the other axis. On the other hand, the most notable variations in the normal stresses are found on the extreme points. However, the amount of the normal stresses over crown surface of the ceramic coated piston, are less than that of conventional piston.

The shear stress distributions versus radial distance for the ceramic coated pistons are shown in Figs 5a and 5b. For thicker ceramic layers, the shear stress reaches its maximum at the edges of the bowl area over the crow region of the piston (Fig 1c). Shear stress is also found much higher on the axis of pin-holes (along line AB), rather than the other axis. According to the results, the shear strength of the ceramic is the prominent factor for selection of coating thickness.

It is noted that, on the internal parts of considered piston, multi-axial stresses are generated because of the complex geometry and thermo-mechanical loading. Therefore, von Mises stress is used as a combined normal stress. The gradients of von Mises stress distribution for the conventional uncoated piston and ceramic coating piston are shown in Figs 6. The maximum von Mises stress of uncoated piston occurred on upper parts of the two pin holes. The calculation results show that the von Mises stress of uncoated piston, are greater than that of ceramic coated pistons at the ring grooves and piston pin holes.

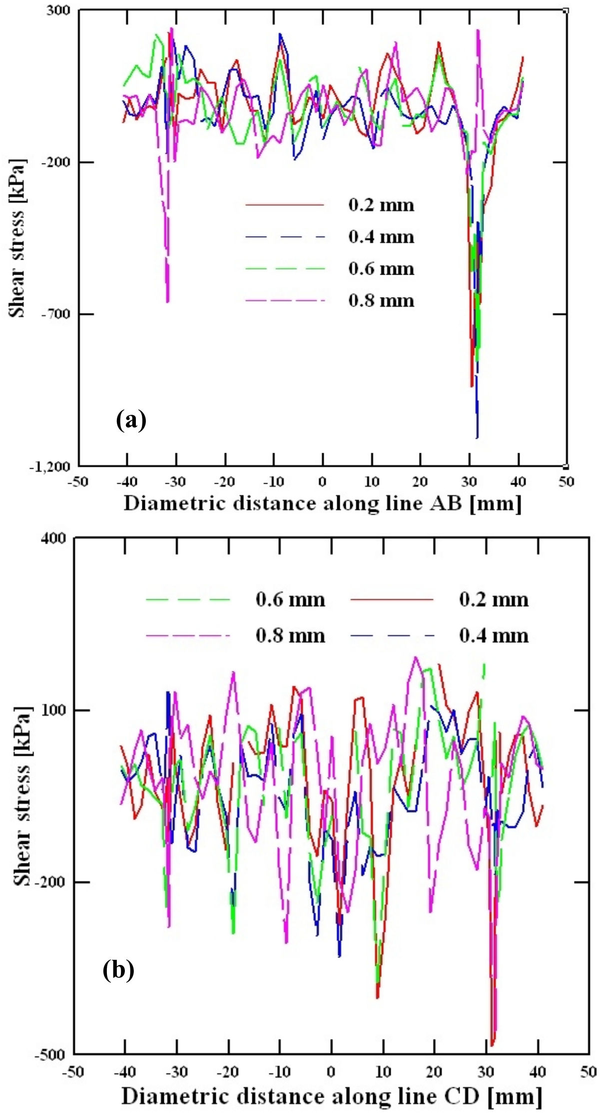


Figure 5: Variation of shear stresses along axes AB and CD over the piston crown surface

Variation of maximum von Mises stress versus the thickness of ceramic layer deposited on the piston crown surface is shown in Fig 7. It is clear that the ceramic coatings can effectively reduce the combined bearing stress of the piston over the pin-hole areas. The relation between the maximum von-Mises stress and the ceramic layer thickness is also found to be a convex curve by ref. [13]. This reduction can notably increase the strength of the piston against crack nucleation and fatigue failure on this region.

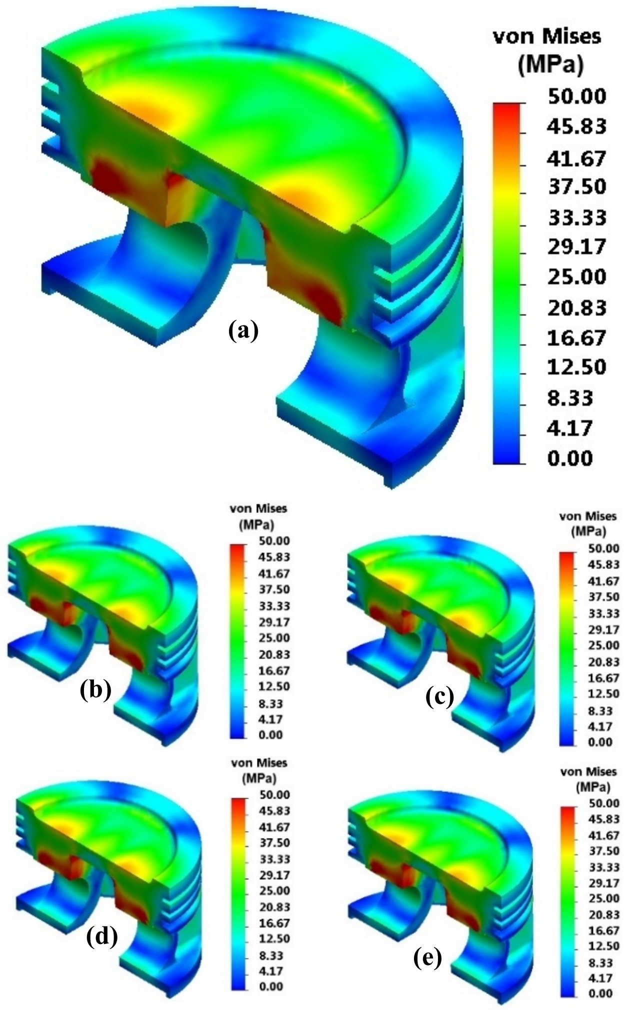


Figure 6: Von Mises stress contours on a) uncoated and ceramic coated pistons: the considered coating thicknesses are b) 0.2, c) 0.4, d) 0.6 and e) 0.8 respectively

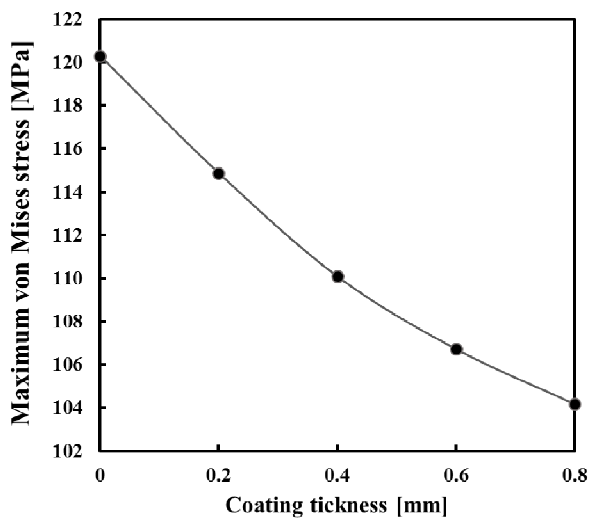


Figure 7: Maximum von Mises stress variation with the coating thickness

The temperature of lubricating oil may be another contributing parameter for improving the intensity of the piston stress and deformation fields. For three different temperatures of $90^{\circ}C$, $80^{\circ}C$ and $70^{\circ}C$ the contours of normal stress, shear stress and von Mises stress are shown in Figures 8, 9 and 10, respectively. To be more accurate, variation of normal and shear stresses along the diametric line of the piston crown are depicted in Figures 8, 9 and 10, respectively.

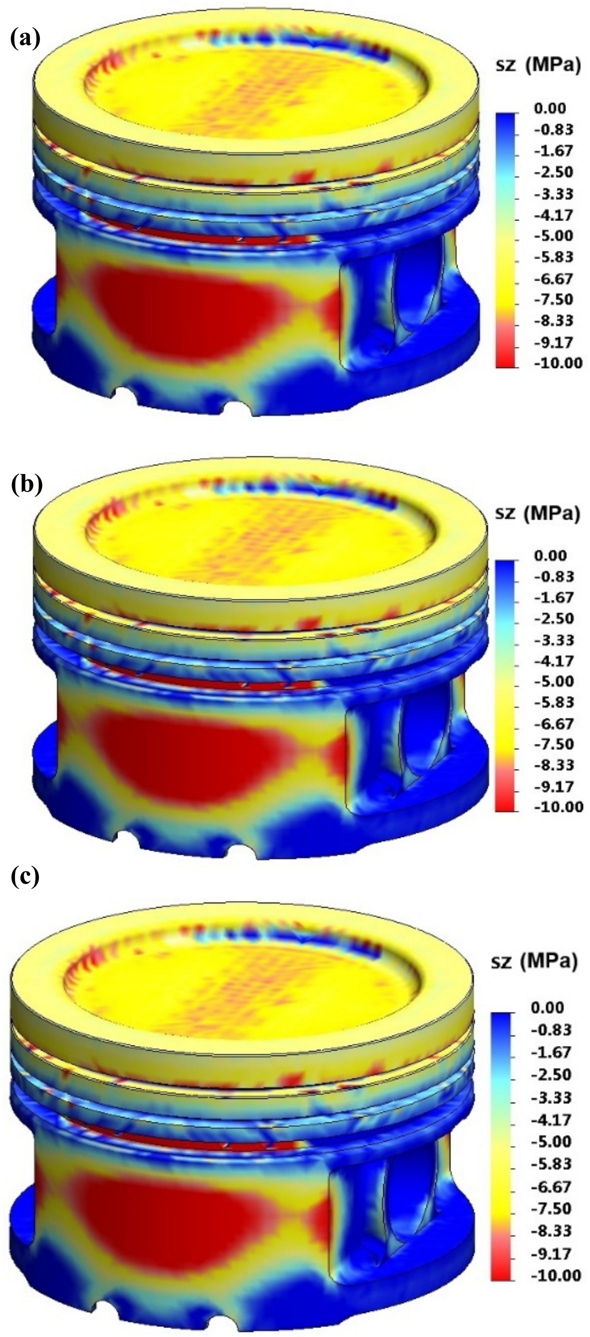


Figure 8: The normal stress gradients of uncoated piston for three different temperature of lubricating oil: a) 70, b) 80 and c) 90.

To be more accurate, variation of normal and shear stresses along the diametric line of the piston crown are depicted in Figures 11a and 11b respectively.

According to the obtained results, the oil temperature has not a considerable effect on thermal stress gradient of the piston.

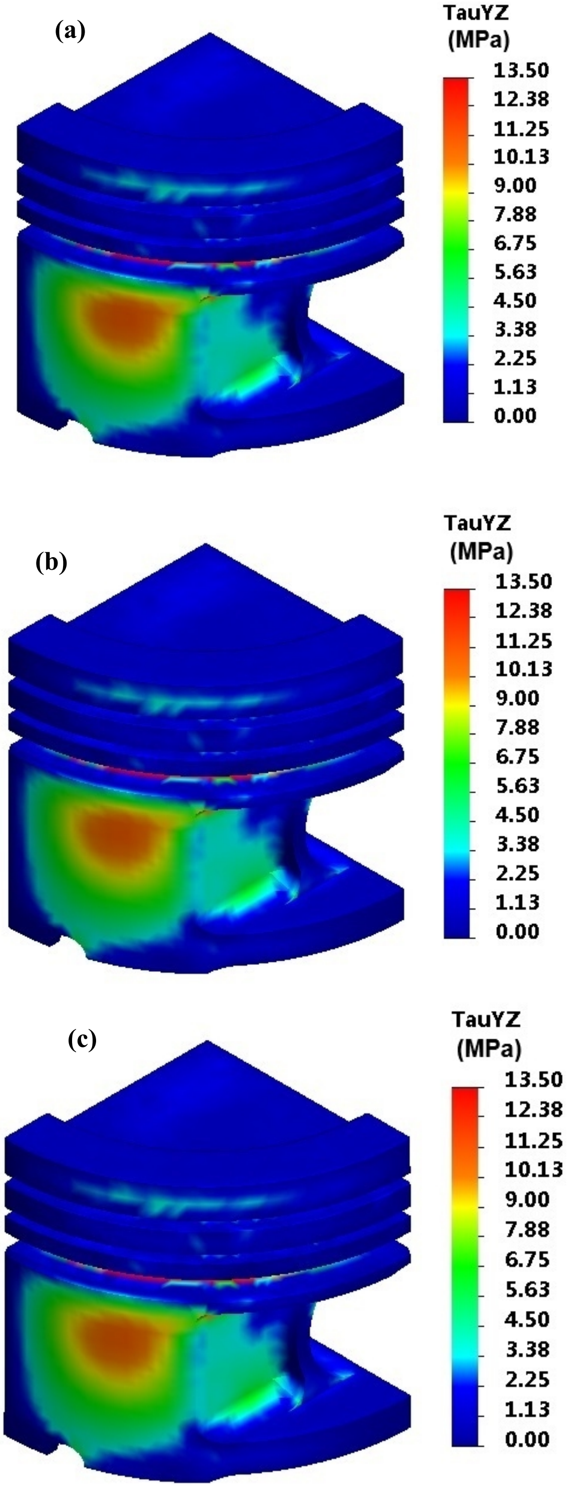


Figure 9: The shear stress gradients of uncoated piston for 3 different temp. of lubricating oil: a) 70, b) 80 c) 90 ℃

As can be seen in Fig 12, the radial displacement of points located on the skirt region can be effectively controlled by lowering the oil temperature. According to the obtained results, if the average temperature of circulating oil is lowered by 10 ℃ , the displacement of entire points located on line EC (Fig. 1b) are decreased by 20%.

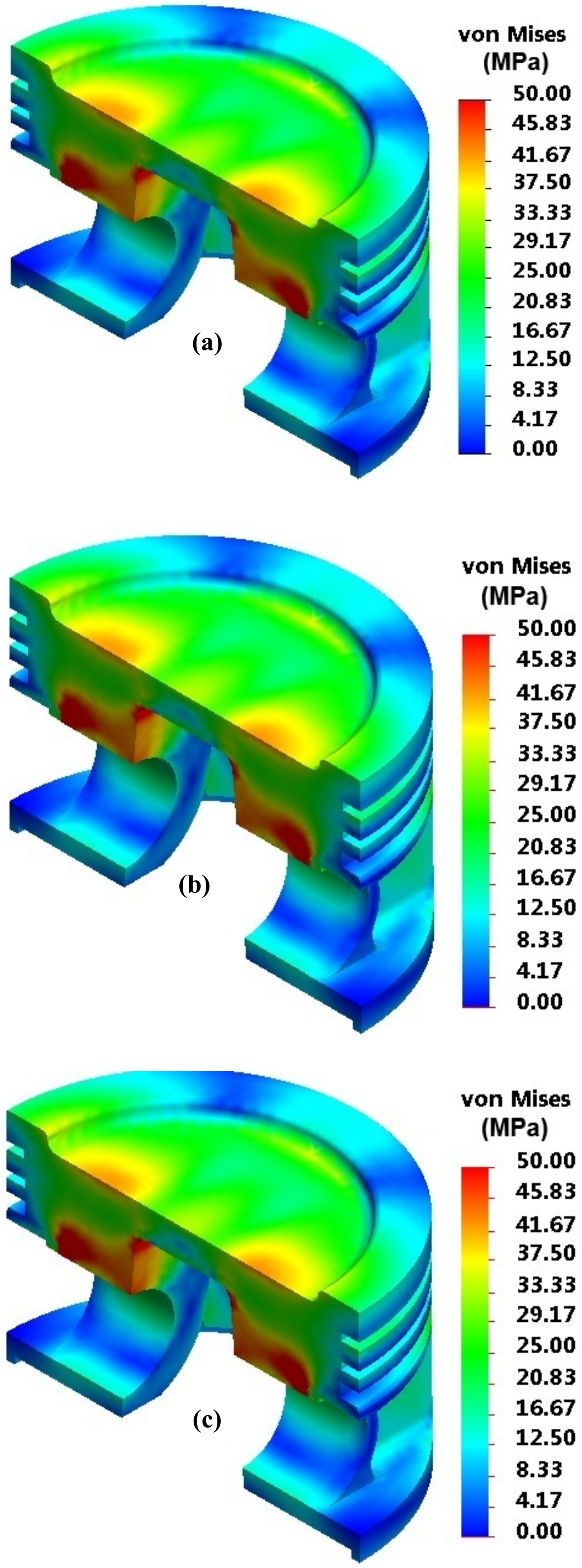


Figure 10: The variation of von Mises stress for three different temp. of lubricating oil: a) 70, b) 80 and c) 90 ℃

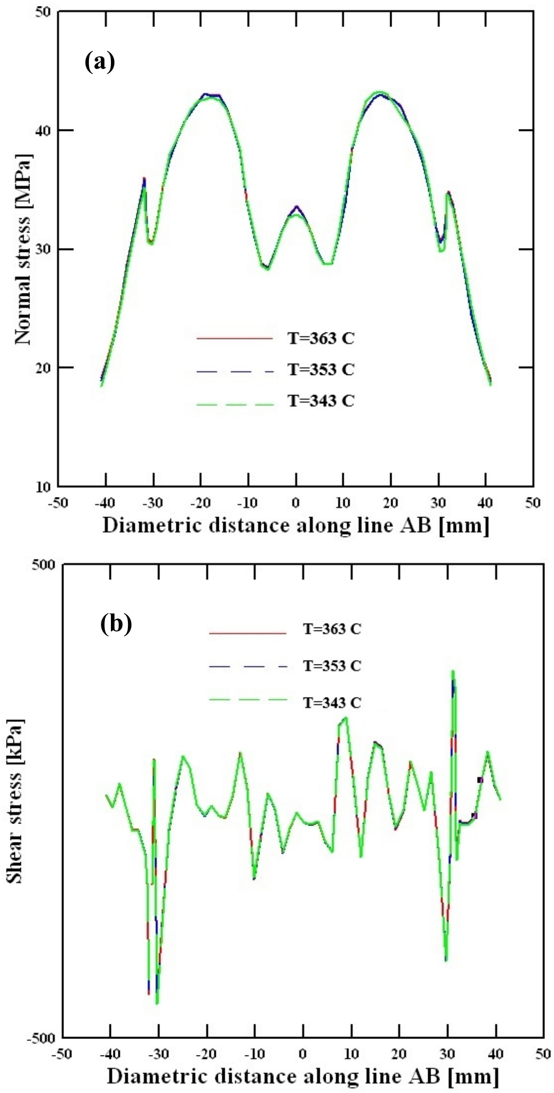


Figure 11: The effect of lubricating oil temperature on variation of stresses on piston crown surface: a) for normal stress, b) for shear stress

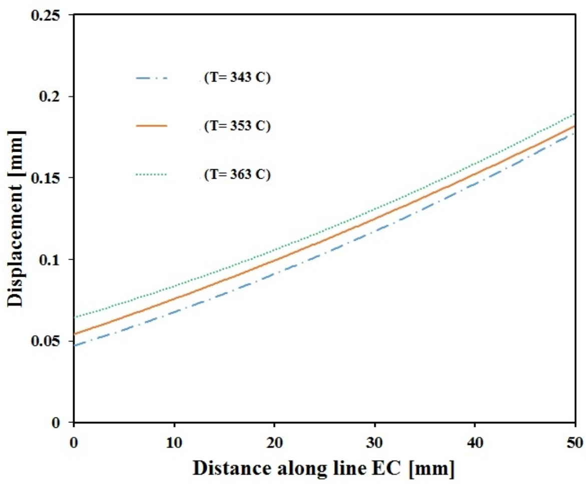


Figure 12: The effect of lubricating oil temperature on radial displacement of the points located on the skirt region of the piston

For different thicknesses of ceramic coating layer, variation of radial displacement of points located on line EC are given in Fig. 13. It is obvious that the lower parts of piston skirt are not affected by the thickness of ceramic layer. However for the points located near the piston crown, the thickness has a considerable effect on controlling the radial expansion of the piston.

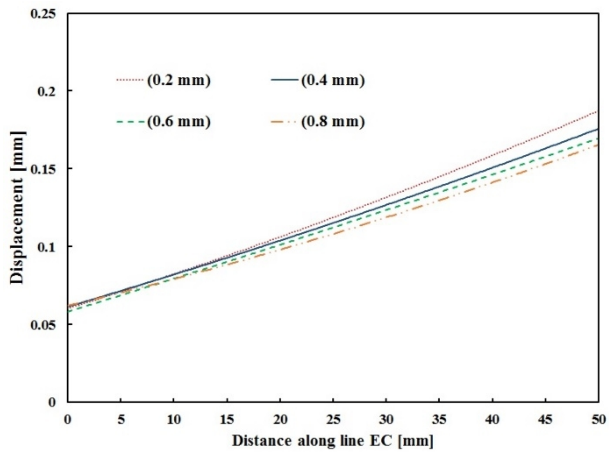


Figure 13: The effect of ceramic coating thickness on radial displacement of the points located on the skirt region of the piston

## 4) Conclusion

In this paper, thermo-mechanical the stress distribution of an aluminum piston is investigated through finite element analysis. The effect of ceramic coating and thermal condition of lubricating engine oil are studied and compared with the results of the uncoated piston. According to the results, the maximum normal stress takes place at the middle surface of the ceramic coating in radial direction. When the coating thickness increases gradually, it moves towards the inner edge of the coating. The maximum stress can be readily controlled by increasing the thickness of ceramic layer. The von Misses stress, which is found critical on upper parts of the pin-hole area, decreases with increasing coating thickness. The shear stress which causes lateral cracks increases with the coating thickness increase and reaches its maximum level at the inner edge of the coated region at the interface of the substrate. According to the obtained results, the temperature of lubricating oil has not a considerable effect on thermal stress gradient of the piston. However, the radial displacement of points located on the skirt region can be effectively controlled by lowering the oil temperature.

## References

[1] E. Buyukkaya, M. Cerit, Thermal analysis of a ceramic coating diesel engine piston using 3-D finite element method, Surface and Coatings Technology, Vol. 202, No. 2, pp. 398-402, 2007

[2] H. Kim, C. Kim, W. Bae, S. Han, Development of optimization technique of warm shrink fitting process for automotive transmission parts (3D FE analysis), Journal of materials processing technology, Vol. 187, pp. 458-462, 2007
[3] O. Singh, Y. Umbarkar, T. Sreenivasulu, E. Vetrivendan, M. Kannan, Y. Babu, Piston seizure investigation: Experiments, modeling and future challenges, Engineering Failure Analysis, Vol. 28, pp. 302-310, 2013
[4] T. M. Yonushonis, Overview of thermal barrier coatings in diesel engines, Journal of Thermal Spray Technology, Vol. 6, No. 1, pp. 50-56, 1997.
[5] A. I. H. Committee, ASM Handbook–Volume 1: Properties and Selection: Irons, Steels, and High Performance Alloys, ASM International, pp. 950-980, 1990
[6] M. Cerit, H. S. Soyhan, Thermal analysis of a combustion chamber surrounded by deposits in an HCCI engine, Applied Thermal Engineering, Vol. 50, No. 1, pp. 81-88, 2013
[7] C.-H. Li, Piston thermal deformation and friction considerations, SAE Technical Paper, 1982
[8] M. T. Abbes, P. Maspeyrot, A. Bouif, J. Frene, A thermomechanical model of a direct injection diesel engine piston, Proceedings of the Institution of Mechanical Engineers, Part D: Journal of Automobile Engineering, Vol. 218, No. 4, pp. 395-409, 2004
[9] S. V. Bohac, D. M. Baker, D. N. Assanis, A global model for steady state and transient SI engine heat transfer studies, 0148-7191, SAE Technical Paper, 1996
[10] A. Ghasemian Moghadam, S. A. Jazayeri, Reducing of Transient Warm-up Period in an Internal Combustion Engine by Preheating of Engine Parts, The Journal of Engine Research, Vol. 17, No. 17, pp. 15-27, 2010
[11] J. Gharloghy, A. H. Kakaee, Thermal Analysis of an SI Engine Piston Using Different Thermal Model, The Journal of Engine Research, Vol. 17, No. 17, pp. 28-41, 2010
[12] R. Pourhamid, H. Mahdavy Moghaddam, A. Mohammadzadeh, Thermal analysis of functionally graded materials in cylinders and pistons based on super element method, The Journal of Engine Research, Vol. 30, No. 30, pp. 25-36, 2013
[13] M. Cerit, M. Coban, Temperature and thermal stress analyses of a ceramic-coated aluminum alloy piston used in a diesel engine, International Journal of Thermal Sciences, Vol. 77, pp. 11-18, 2014
[14] M. Cerit, Thermo mechanical analysis of a partially ceramic coated piston used in an SI engine, Surface and coatings Technology, Vol. 205, No. 11, pp. 3499-3505, 2011
[15] A. Gilbert, K. Kokini, S. Sankarasubramanian, Thermal fracture of zirconia–mullite composite thermal barrier coatings under thermal shock: A numerical study, Surface and Coatings Technology, Vol. 203, No. 1, pp. 91-98, 2008
[16] J. E. Shigley, C. R. Mischke, T. H. Brown, Standard handbook of machine design: McGraw-Hill New York, 1986
[17] G. F. Hohenberg, Advanced approaches for heat transfer calculations, 0148-7191, SAE Technical paper, 1979
[18] G. Woschni, A universally applicable equation for the instantaneous heat transfer coefficient in the internal combustion engine, 0148-7191, SAE Technical paper, 1967
[19] G. Garbinčius, V. Bartulis, R. Pečeliūnas, S. Pukalskas, The influence of coolant scale deposit inside the internal combustion engine on the piston and cylinder deformations, Transport, Vol. 20, No. 3, pp. 123-128, 2005
[20] E. Buyukkaya, Effects of thermal barrier coating on a turbocharged diesel engine exhaust emissions, Sakarya University, Mechanical Engineering Department, Ph D. thesis, Institute of Sciences and Technology, Turkey, 1997
[21] V. Esfahanian, A. Javaheri, M. Ghaffarpour, Thermal analysis of an SI engine piston using different combustion boundary condition treatments, Applied Thermal Engineering, Vol. 26, No. 2, pp. 277-287, 2006
[22] X.-B. Liu, M. Pang, Z.-G. Zhang, J.-S. Tan, G.-X. Zhu, M.-D. Wang, Numerical simulation of stress field for laser thermal loading on piston, Optics & Laser Technology, Vol. 44, No. 5, pp. 1636-1640, 2012.
[23] M. Nazoktabar, R. Mehdipour, Z. Baniamerian, SIMULATION OF BOILING HEAT TRANSFER WITHIN WATER JACKET OF 4-CYLINDER GASOLINE ENGINE (TECHNICAL NOTE), International Journal of Engineering-Transactions C: Aspects, Vol. 27, No. 12, pp. 1928, 2014
[24] A. Tarasov, T. Kolina, S. Shalaginov, Thermal spraying of coatings on piston rings of diesel engines, Welding international, Vol. 14, No. 4, pp. 301-304, 2000
[25] W. Ostapski, Analysis of thermo-mechanical response in an aircraft piston engine by analytical, FEM, and test-stand investigations, Journal of Thermal Stresses, Vol. 34, No. 3, pp. 285-312, 2011
[26] L.-Y. Feng, X.-Y. Gao, H.-M. Xia, F. Xu, The coupled thermal and mechanical load analysis in the 8 E 160 type diesel's piston assembly, Transactions of Chinese Society for Internal Combustion Engines, Vol. 20, No. 5, pp. 441-446, 2002
[27] Y. Wang, Y. Dong, Y. Liu, Simulation Investigation on the Thermo-mechanical Coupling of the QT 300 Piston, in Proceeding of, IEEE, pp. 77-80
[28] B. Zhao, Thermal stress analysis of ceramic-coated diesel engine pistons based on the wavelet finite-element method, Journal of engineering mechanics, Vol. 138, No. 1, pp. 143-149, 2011

فصلنامهٔ علمی- پژوهشی تحقیقات موتور

تارنمای فصلنامه: www.engineresearch.ir

# برآورد تنش‌های هم‌زمان حرارتی و مکانیکی سنبه آلومینیمی موتور بنزینی ایکس یو هفت

حسین گلبخشی[1*]، مسلم نامجو[2]، مجید دولتی[3]، فرهاد خوشنام[4]

*[1و2و3و4] دانشگاه جیرفت، جیرفت، ایران*

*نویسندهٔ مسئول، golbakhshi@ujiroft.ac.ir

## چکیده

در موتورهای جدید که از نسبت تراکمهای بالاتری برخوردار هستند، قطعات موتور تحت فشار و حرارت ناهمگن شدیدتری قرار می گیرند. سنبه به عنوان یکی از بحرانی ترین قطعات موتور همواره موضوع اصلی در بسیاری از تحقیقات مرتبط با تعیین توزیع دمایی بوده است. با این وجود، تحقیقات محدودی در زمینه تعیین تنش ها در این قطعه انجام شده است. در بررسی حاضر، سنبه موتور بنزینی ایکس یو هفت که کاربرد فراوانی در صنعت خودروی ایران دارد مورد تحلیل حرارتی و مکانیکی قرار گرفته است. مدل اجزاء محدود سه بعدی مبتنی بر تحلیل الاستیک خطی در محیط نرم افزار COSMOS Works ارائه شده است تا به کمک آن امکان برآورد توزیع تنش های حرارتی در مرحله احتراق فراهم شود. حداکثر تنش قائم در مرکز تاج سنبه و مقدار بحرانی تنش وان میسز در قسمت های بالایی سوراخ محور سنبه مشاهده گردید. تاثیر ضخامت لایه سرامیکی پوششی بر توزیع تنش ایجاد شده در سنبه محاسبه و با نتایج مربوط به سنبه متداول بدون پوشش مقایسه گردیده است. طبق نتایج بدست آمده، حداکثر بزرگی تنش ها را به طور مؤثری می توان با افزایش ضخامت لایه سرامیکی کنترل نمود.



## اطلاعات مقاله

*تاریخچهٔ مقاله:*
دریافت: ۵ آبان ۱۳۹۴
پذیرش: ۲۵ اسفند ۱۳۹۴

*کلیدواژه‌ها:*
سنبه
اجزاء محدود
تحلیل ترمو-مکانیکی
پوشش سرامیکی
توزیع تنش